Prepared for submission to JINST

An instrument for measuring T-odd asymmetries in the fission of heavy nuclei

D. Berikov,[a,f,1] **V. Hutanu,**[e,2] **Yu. Kopatch,**[a,b] **G. Ahmadov,**[a,g,h] **A. Gagarski,**[c] **V. Novitsky,**[a,b] **G. Danilyan,**[a,b] **S. Masalovich,**[d] **J. Klenke,**[d] **and H. Deng**[e]

[a] *Joint Institute for Nuclear Research, Joliot-Curie 6, 141980 Dubna, Russia*

[b] *Institute for Theoretical and Experimental Physics of National Research Centre "Kurchatov Institute", 25, Bol'shaya Cheremushkinskaya str., 117218 Moscow, Russia*

[c] *Petersburg Nuclear Physics Institute of National Research Centre "Kurchatov Institute", Gatchina 1, 188300 Leningradskaya Oblast, Russia*

[d] *Heinz Maier-Leibniz Zentrum (MLZ), Technical University of Munich, Lichtenbergstr. 1, 85748 Garching, Germany*

[e] *Institute of Crystallography, RWTH Aachen and Jülich Centre for Neutron Science at Heinz Maier-Leibnitz Zentrum (MLZ), Lichtenberg str. 1, 85748 Garching, Germany*

[f] *L.N. Gumilyov Eurasian National University, Satpayev Str., 2, 010008 Nur-Sultan, Kazakhstan*

[g] *Azerbaijan National Academy of Sciences- CSSR and IRP, 9, B.Vahabzade Str., AZ1143 Baku, Azerbaijan*

[h] *National Nuclear Research Center, Inshaatchilar 4, AZ1073 Baku, Azerbaijan*

E-mail: daniyar.berikov@gmail.com, Vladimir.Hutanu@frm2.tum.de

Abstract: We describe an experimental setup used to measure the T-odd asymmetry effects for prompt fission neutrons and γ-rays in binary fission of some heavy nuclei induced by polarized neutrons with resonance energy. The overall setup as well as the details of the design and performance of the key components like fission fragment detectors, neutron and γ detectors, and the electronics used in the data acquisition and processing system are presented. The experimental setup on beam line POLI of the FRM-2 reactor (Garching, Germany), as well as the neutron beam characteristics, polarization measurements are described, too.

Keywords: Instrumentation for neutron sources; Instrumentation and methods for heavy-ion reactions and fission studies; Neutron monochromators and transport; Polarisation; Neutron detectors (cold, thermal, fast neutrons); Gamma detectors; Modular electronics; Data acquisition circuits.

[1] Corresponding author.
[2] Corresponding author.

Contents

1 Introduction

T-odd angular correlation of the captured by nucleus neutron spin σ, the momentum of light (heavy) fission fragment (FF) p_f and ternary particle (TP) p_α of the type:

$$W(\Omega) \sim 1 + < D > \cdot \sigma \cdot [p_f \times p_\alpha]$$

was discovered in an angular distribution of fission products for ^{233}U ternary fission induced by cold polarized neutrons [1, 2]. The initial aim of that experiment was to search for violation of time reversal invariance (TRI) following the idea, proposed in [3], where the similar correlation $(\sigma \cdot [p_e \times p_\nu])$ was explored for check of the TRI in neutron beta-decay. The experimental value of $< D >$ coefficient was found unexpectedly high, about 10^{-3}. The discovered effect (the asymmetry) could not be indisputable assign to the evidence of the TRI violation. The reason is related to the significant influence of the interaction between fission products in final states and as well the interference of reaction amplitudes of neighboring compound states. The result of these investigations caused the discovery of T-odd asymmetries of the TRI and ROT types in the ternary fission of a number of actinide nuclei [4–6]. Both effects (TRI, ROT), being formally T-odd, currently are not considered as violating the time reversal invariance. They are explained by the complicated mechanism of the fission processes. By measuring these effects one can obtain unique information about the total angular momentum J and K (its projection on the deformation axis), which characterize the fission channels introduced by A. Bohr. Up to now, all measurements of the T-odd effects were performed for the cold neutron induced fission, where several fission channels are mixed with unknown weights [7].

It is very necessary to carry out measurements with different incident neutron energies in order to figure out different spin states and get "clean" data on the J and K channel weights. One such experiment was performed at the POLI instrument (the FRM-2 reactor in Garching) which provides the polarized neutron beam with desirable energies. The schematic view of the experimental setup at the POLI instrument is depicted in figure 1. Details of these measurements may be found elsewhere [8].

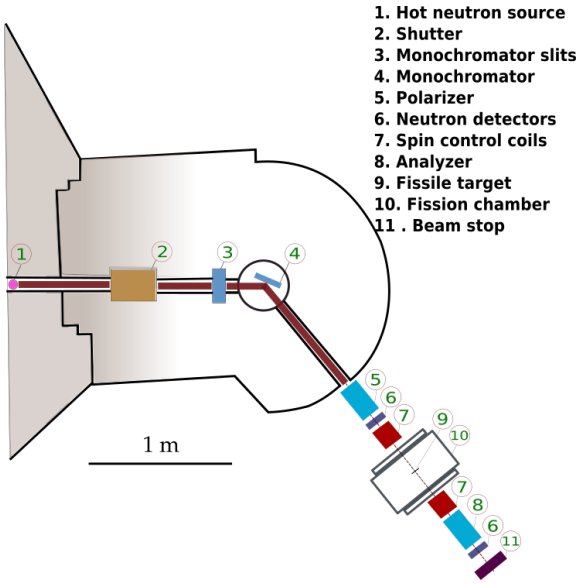

Figure 1. Schematic view of the experimental setup with POLI instrument at MLZ.

The focus of this article is on the description of the instrumental setup. We describe the hot neutron beam line, neutron polarization and analyzing method, the spin transport and manipulation, fission chamber and detectors and provide the efficiency prove.

2 Hot neutron beam

We used the polarized hot neutron beam with a short wavelength provided by POLI diffractometer at the FRM-2 reactor at the Maier-Leibnitz Zentrum in Garching (Germany) [9–11]. On POLI Cu-mosaic and Si-perfect crystal, variable double-focusing monochromators are employed to produce an intense monochromatic beam of required energy, and additionally ^3He spin filter cells to polarize the beam or analyze the polarization [12]. This method offers the best performance in the polarization of hot neutrons. The decoupling of polarization and neutron optical properties increases the flux of polarized neutrons more than twice comparing to the Heusler crystal polarized monochromator, due to possibility of better focusing the neutron beam [13]. There is a possibility to work at four different wavelengths between 0.55 and 1.15 $\dot{A}$ using Cu (220), and Si (311) focusing monochromators and resonance $\lambda/2$ filters. The available wavelength as well as the estimated flux densities at the sample position are summarized in Table 1.

Table 1. Primary beam: SR-9a on the hot source FRM-2. Double-focusing monochromators POLI. Estimated values for the maximal non-polarized neutron flux are noted.

Crystal (reflection)	Monochromator take-of angle $2\theta_M$					
	25°			41°		
	Wavelength [$\dot{A}$]	Energy [meV]	Flux $[n(sm^2)^{-1}]$	Wavelength [$\dot{A}$]	Energy [meV]	Flux $[n(sm^2)^{-1}]$
Cu (220)	0.55	270	$7{\cdot}10^6$	0.9	101	$1.2{\cdot}10^7$
Si (311)	0.7	167	$8.5{\cdot}10^6$	1.15	62	$1.8{\cdot}10^7$

3 Neutron polarization

3.1 Spin filter cells and magnetostatic cavities

The incoming beam was polarized by means of ^3He spin filter cell (SFC). The same type of cell was also used as an analyzer for measuring beam polarization. Since polarized nuclei of ^3He possess very high spin-dependent neutron absorption efficiency over a wide range of energies, the ^3He cell can be used as a broadband neutron polarizer or analyzer. It is possible to optimize its efficiency for nearly all neutron wavelengths by tuning the gas pressure in the cell. SFC as well as the compact magnetostatic cavities specially designed and built for the use at POLI [14, 15]. Spin filter cells are optimized to maximize the quality factor Q, defined as $Q = P^2T$, where P is the neutron polarization and T is the neutron transmission of the filter. The dimensions of the standard POLI cells are 60 mm in diameter and 130 mm inner length. The typical thickness of the windows is 3-4 mm. Working pressure can be chosen up to 3 bar, while the bursting pressure is not less than 5 bar. One of the cells is shown in figure 2. It is made of HOQ 310 quartz glass and is coated with Cs.

Figure 2. Refillable Cs-coated spin filter cell, made of fused silica.

The cell should be placed in a homogeneous magnetic guide field in order to maintain the ^3He polarization in a polarizer or analyzer. Mu-metal magnetic shields were used to assure the stability of the guide field in the presence of moderate magnetic stray fields [15]. The photograph of the magnetostatic cavity with a spin filter cell inside is shown in figure 3. The precise design of the

compact magnetostatic box including magnetic field simulations are going to be published in a dedicated report. The outer dimensions of the box are $(L \times B \times H)$ $320 \times 206 \times 100mm$. Magnetic field inside the box: 5-10 Oe. The typical relaxation time constant $T1$ obtained in such very compact cavity with large windows for neutron beam is about 40 h. This requested daily replacement of the SFC with freshly polarized gas from Helios MEOP station [12].

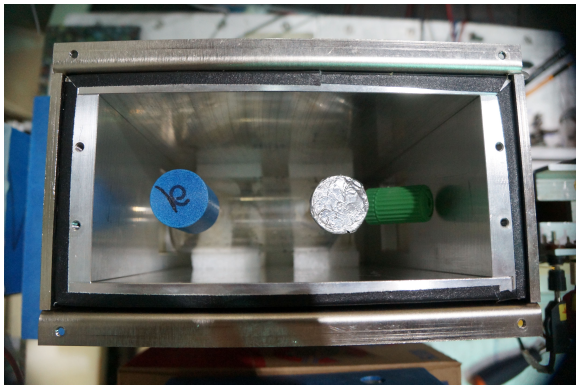

Figure 3. Spin filter cell inside the compact magnetostatic cavity.

3.2 Transmission measurement of the SFC

The empty quartz glass cells give a transmission between 0.85 and 0.88 for a neutron wavelength of 0.55 $\dot{A}$. This value changes depending on the thicknesses of windows. The polarization of the incoming beam was determined by the transmission measurement of the SFC using two beam monitors [16]. The following formulas described a relationship between the transmittance (T) of a spin-filter for an incident unpolarized monochromatic neutron beam and neutron polarization (P):

$$T = T_0 \cdot e^{-\eta} \cdot cosh(\eta P_{He}) \tag{3.1}$$

$$P = tanh(\eta P_{He}) \tag{3.2}$$

Here T_0 is a neutron beam transmission measured for an evacuated SFC cell and P_{He} the polarization of the ^3He gas used. It can be easily determined from the transmission measurement (3.1) for known parameter - η. And then, substituted in 3.2, the neutron polarization at certain time point can be calculated. The η defines a filter opacity. The opacity is directly related to the σ_0, σ_p, N, and d, where N is the number of atoms per unit volume, d the filter thickness, σ_0 the spin-independent part of the total cross-section and σ_p is the so-called polarization cross-section. The value of the opacity of the ^3He gas could be estimated for practical purposes at room temperature as:

$$\eta = 7.32 \cdot 10^{-2} \cdot p(bar) \cdot d(cm) \cdot \lambda(\dot{A}) \tag{3.3}$$

where p is the gas pressure, d the neutron path length in the gas and λ the neutron wavelength. For clarity, the dependence of the transmission and the degree of neutron polarization on the degree of polarization of the ^3He was determined based on experimental results and equations 3.1 - 3.2. These dependencies for 0.55 $\dot{A}$ neutrons calculated for the 13 cm long SFC filled with 2.5 bar are plotted in figure 4. Further, increasing of the polarizer efficiency in the future may be reached by using cells with higher opacity and magnetostatic cavities with longer relaxation times.

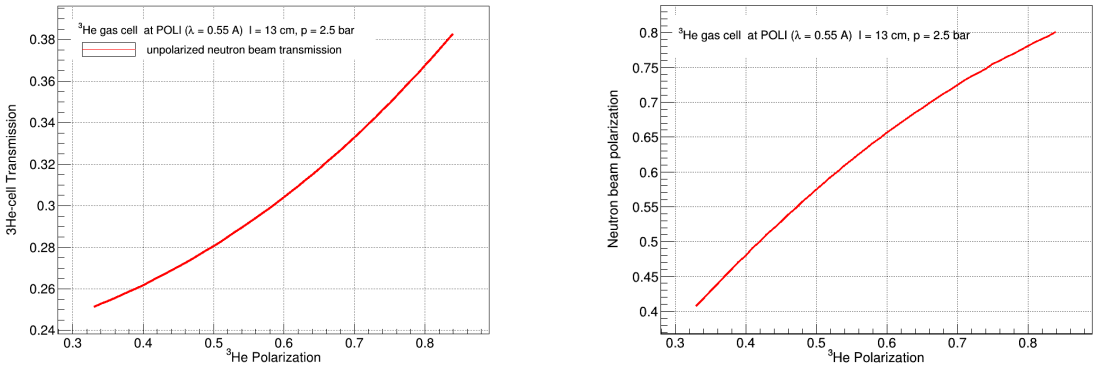

Figure 4. Dependence of the transmission and polarization of neutrons on the degree of polarization of the 3He gas in the SFC.

3.3 Spin transport and manipulation

Both polarizer and analyzer provide vertical polarization of the neutron beam while the searched effect requires horizontal polarization (forwards and backwards along the beam propagation direction). Both spin turn into required direction and spin-flip parallel/antiparallel to the beam propagation are required between the polarizer and fission chamber. Moreover, external parasitic stray fields, unavoidably present under the real experimental environment, may partially depolarize the neutron beam over the Larmor precession around those fields. For example, a magnetic field of only 0.5 Oe (comparable to the Earth's magnetic field in the range 0.25 - 0.65 Oe) can lead to a spin rotation of 21° at a distance of only 30 cm from the polarizer for neutrons with the energy of 0.3 eV. The farther away the devices for flipping the spin of polarized neutrons from the object under study are located, the greater the probability of depolarization. In order to preserve the polarization vector orientation of the neutron beam, on the one side, the distance of pass in the uncontrolled magnetic surrounding should be minimized, on the other side, some compensation coils to correct for the appeared precession may be used. In order to satisfy all mentioned requirements dedicated compact-size spin-control device was designed and built. The detailed description including magnetic field calculations for this device will be published in a dedicated report. Here we only briefly present its principle of operation and approximated design. Two similar devices have been used in immediate vicinity to the fission chamber: one between polarizer and fission chamber to control the incoming polarization vector and another one after the fission chamber before the analyzer in order to monitor the polarization value and calibrate the setup (figure 5).

A spin-control device is an assembly of three identical rectangular planar precession coils independently powered by a DC power supply (figure 6). Each coil is wound on a rectangular body with side-grooves made to ensure high precision wiring of 1 mm aluminum wire with a thin electrically insulating coating to avoid shorts between the wires. The used wire has low neutron absorption and scattering cross-section. The coil body was made of polyamide and has wiring section of 70 × 70 mm^2 of 65 turns. The first coil serves as a spin rotator and flipper with filed axis lying in the horizontal plane perpendicular to the direct beam. The incoming vertical polarization precesses around the field by 90° toward the beam propagation direction. By flipping

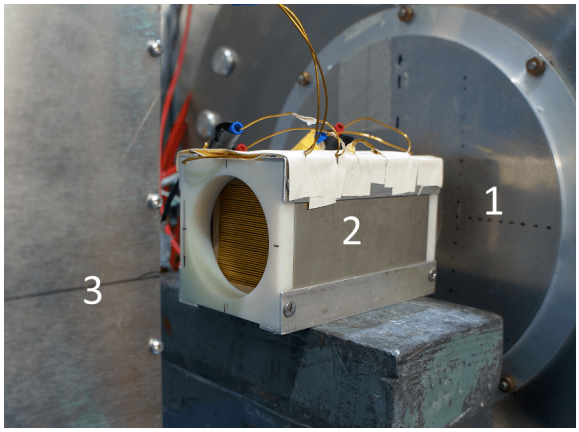

Figure 5. Spin control device (2) placed between fission chamber (1) and analyzer (3).

the field direction in the coil spin is turned backwards to the beam propagation. Thus, the incoming polarization is flipped by 180° every 1.3 seconds. The remaining two coils serves to compensate for the effects of external fringe magnetic fields on polarization and to correct for any imbalance in the total magnetic field integral. This is done by scanning the current in the coils and setting it value to the maximum polarization of the neutron beam. Figure 7 shows the experimental dependence of the detector counting rate on the current in the correction coils. The coils were yoked in 2 mm thick high permeability ferromagnetic screen (permalloy) mark 79NM for flux return and reduction of the stray fields.

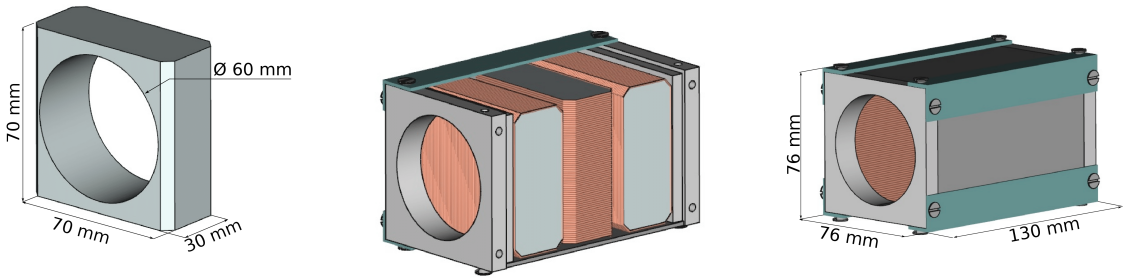

Figure 6. Spin-control devise construction: on the left - coil body made of polyamide, in the middle - the location of the coils inside the ferromagnetic screen, acting as a yoke for the fringe fields, on the right - a general view of the spin-control coils array as described in the text.

4 Fission chamber and detectors

The studied target (^{235}U) was spattered from the both sides on a rectangular Al plate with approx. Dimensions 40×100 mm^2, situated with the long side along the beam direction. The total amount of fissile material in the test experiment was about 82 mg. Other materials or sample sizes are also possible to be used in the described setup. The fission events were recorded by two fragment detectors - low-pressure multiwire proportional counters (LPMWPC), being placed parallel to the target on both sides of it at a distance of 3 cm (start detector) and 11 cm (stop detector) (figure

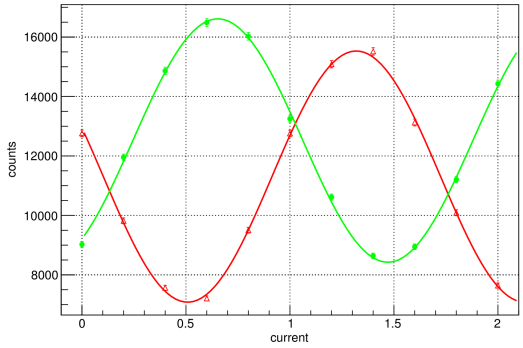

Figure 7. Setup calibration. Dependence of the detector counts on current in the compensation coil. The green curve corresponds to spin-, red curve to spin+. Cosine fit determines the optimal value of near 0.2 A.

8). Each stop counter consists of five independent segments to increase the angular sensitivity of the detector. Basic advantages of LPMWPCs which make them very suitable for registration of heavy ions such as fission fragments (FFs) are: excellent timing characteristics, high efficiency, high transparency and low energy losses inside the detector, large surface area, high counting rate capability, good position resolution with proper signal readout, long term stability. In table 2 typical parameters of LPMWPCs are presented.

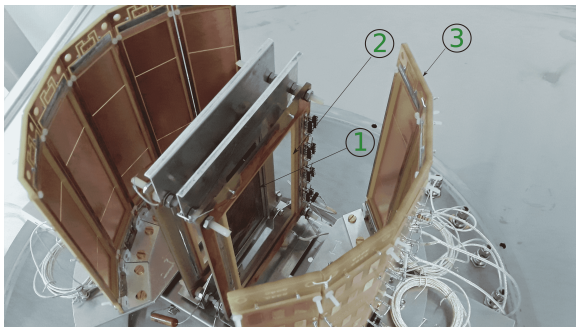

Figure 8. Picture of the low-pressure multiwire proportional counters. 1 - fissile target, 2 - start detector, 3 - stop detector.

LPMWPC detectors work in the tetrafluoromethane environment (CF_4) at a gas pressure of about 10 mbar. To ensure such conditions, the target and two fragment detectors were enclosed in a stainless steel vacuum-proof fission chamber filled with CF_4 gas. In order to avoid neutron depolarization the entrance/output windows of the chamber are made of Al alloy. For precise positioning of the target in the beam, the whole chamber is placed on a remotely controlled motorized rotation and translation stages. The pressure of the gas in the chamber was continuously monitored and in-situ gas/vacuum supply lines are connected to the chamber. Figure 9 shows the photograph of the assembled fission chamber.

Prompt fission γ-ray and neutron detectors are located outside the fission chamber. Each of these detectors is a scintillation counter. As a scintillator, plastic and NaI (Tl) crystals were used, which made it possible to effectively register not only γ quanta, but also neutrons. Eight

Table 2. The typical parameters of LPMWPC.

Working pressure	~ 0.1 - 10 mbar
Counting gases	Isobutane, heptane, ethylene
Anode-cathode gap	~ 1.6 - 3.2 mm
Anode wire spacing	~ 1 mm
Anode wire diameter	~ 10 - 25 μm
Reduced electric field in the constant field region	~ 10^2 - 10^3 V/(cm · mbar)
Reduced electric field on the wire surface	~ 10^4 - 10^5 V/(cm · mbar)
Total gas amplification	~ 10^4 - 10^6
Amplification on the wires	~ 10^1 - 10^3
Signal current pulses rise time	~ 2 - 5 ns
Timing resolution	~ 0.1 - 1 ns

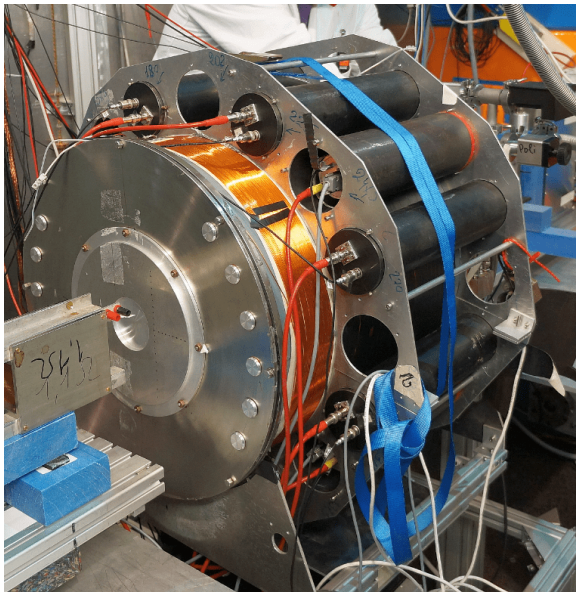

Figure 9. The installed fission chamber. Output Al window is visible on the left side. Gas and vacuum valves are visible in the back side (right upper corner in the picture).

cylindrical plastic scintillators with a diameter of 70 mm and a length of 120 mm, supplied with a photomultiplier EMI 9839A, and four NaI scintillators were inserted in a rotatable holder at a distance of about 30 cm from the target center. Up to 12 detectors worked simultaneously. The schematic view of the used detector array inside/outside the fission chamber is shown in figure 10.

The scintillator detectors ensure subsequent measurements of coincidences of prompt fission γ- rays and neutrons with fission fragments at angles of ±22.5, ±67.5, ±112.5 and ±157.5 degrees with respect to the mean axis of the detection of fragments. Prompt neutrons and prompt γ-rays from fission were separated via plastic scintillators using the time-of-flight technique. The start signal was the signal from the fission fragment detectors, which also served as a trigger indicating the fission event.

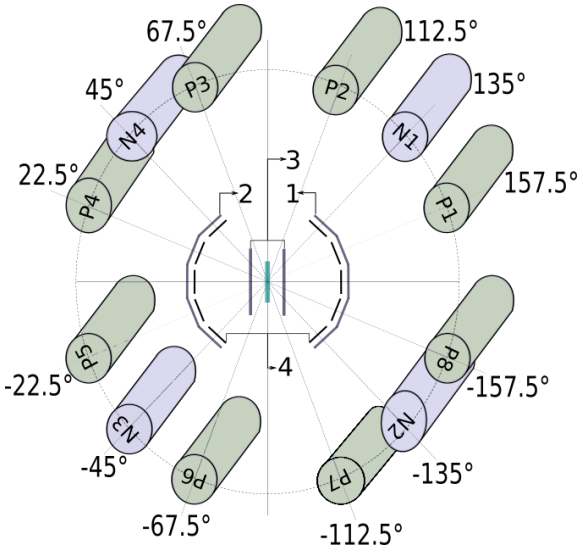

Figure 10. The layout of the detector positioning around the target inside/outside the fission chamber. View from the beam direction. 1 - Stop – cathode 1, 2 - stop – cathode 2, 3 - start – cathode 1+2, 4 - stop – anode 1+2.

5 Data acquisition electronics

The simplified scheme of the data acquisition system (DAQ) is shown in figure 11. The DAQ includes preamplifiers (PAM), timing filter amplifiers (TFA), constant fraction discriminators (CFD) for time pick-up, Time-to-Digital Converters (TDCs), logical modules AND, OR, Logic fan-in/fan-out (FIFO), Analog-to-Digital Converters (ADCs), delays, scaler, and the VME-PC interface running on the Linux operating system. For simplicity, we do not show some modules in the figure. Three signal lines of pulse processing can be identified in figure 11 recording event times on TDC boards, recording pulse heights via ADC and counting events in scaler.

Preamplifiers were used to amplify weak signals from fission fragment detectors. A time filter amplifier (TFA) was used to amplify and properly shape the output pulses provided by the preamplifier. Amplified signals were split such that one output was fed to ADC and another to CFD. The CFD converted the analog signals to logic pulses that were fed to AND/OR logic units. Delayed output signals of CFD were sent to the scaler and TDC. The common start for the TDC, as well as the common gate for the ADC was created from a coincidence of one of the fission fragment detectors and any of the scintillator counters.

Signals from γ-ray and neutron detectors were split and sent to spectroscopic amplifiers and CFDs. Outputs of the spectroscopic amplifiers were delayed and fed to ADC. Shaped output signals of CFDs were split into two parts. The first one was delayed and sent to the scaler and TDC (for stop), while the second one was fed to OR logic gate in order to get a single output for scintillation detectors. This logic and FF logic signals were fed to AND gate in order to provide coincidence between FF and scintillation detectors. The AND gate output was fed to the common gate (G) of ADC, common start of TDC, the scaler, and also sent to logic FIFO 1. A signal from the spin flipper had two components. The first one was produced a few μs before the actual spin flip and lasted about 50 μs. This signal was fed together with the "TDC busy" and "ADC busy" signals to logic

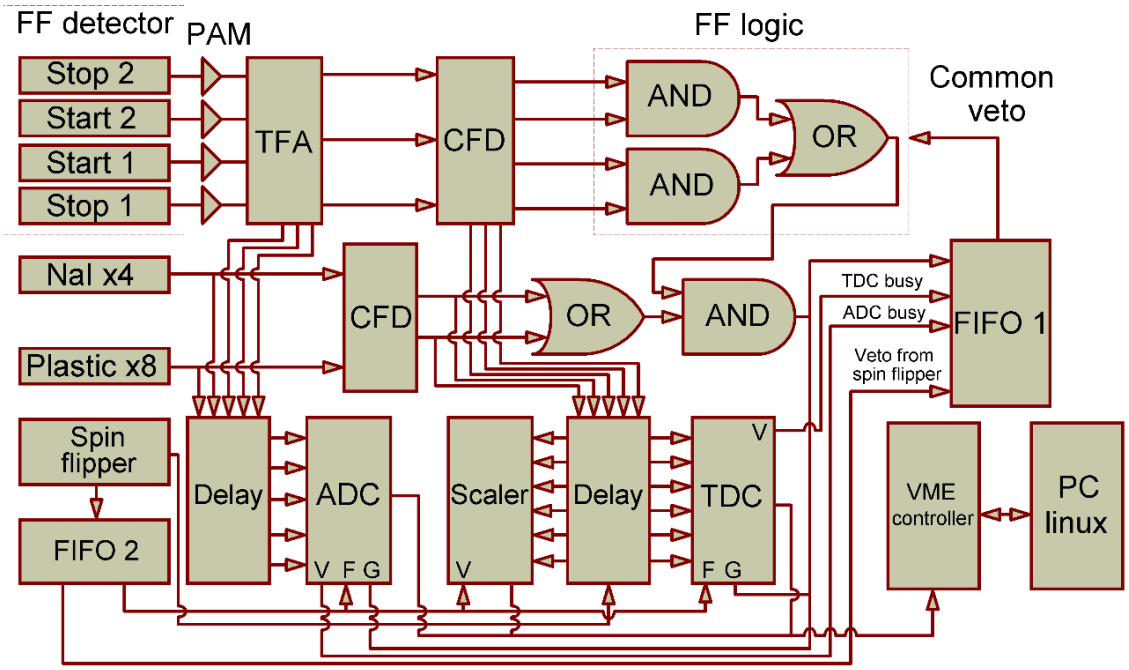

Figure 11. The scheme of the data acquisition system.

FIFO 1 and used to veto the main coincidence unit during the spin flip when the spin orientation could be still unsettled. The second component of the spin flipper signal was produced after the end of the first component and was split into two parts – one for positive and one for negative spin. Both were sent to the SIS3820 VME logic unit and were used for generating interrupts in the PC DAQ software indicating the spin flip condition. The DAQ system was controlled by the PCI/CPI-VME link interface card-SIS1 100/3100 used for subsequent data transfer from the VME buffers to the PC through an optical fiber.

The program reads data from the scaler after each neutron spin flip. These data were used to monitor the status of the setup and instrumental asymmetry. The frequent (about 1.3 Hz) spin flip of the incident neutron beam served as one of the main mechanisms for suppressing instrumental asymmetry. Therefore, special attention was paid to the stability of the measurement time for opposite values of the neutron spin. The scaler controlled the data acquisition time with an accuracy of 10^{-6} sec. For each triggered event (coincidence between one of the FF detectors and one of the γ-ray/neutron detectors) the data from the TDC and ADC were stored as list-mode-data together with the information about the spin sign. During one day of measurements, about 5 GB of compressed data was collected, divided into 5-minute expositions, which were then analyzed off-line. An example of the obtained time-of-flight spectrum is shown in figure 12.

The DAQ allowed increasing the coincidence rate using only "start" FF detectors. This was tested in our last measurement in which ROT effect was studied. This made the determination of the fragment mass (separation of light and heavy fragment groups) impossible and increases the angular spread of the fission fragments. For the ROT-effect however, the light-heavy fragment separation is not necessary since the effect is mass-symmetric. Thus, the use of the "start" detector

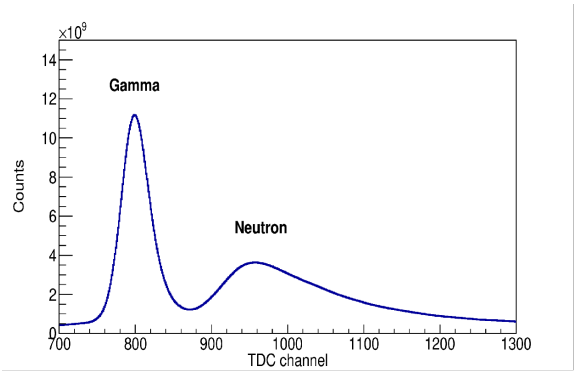

Figure 12. Time-of-flight spectrum from one of the plastic detectors.

only, increases the solid angle of the FF detection on the one side, which could lead to a decrease of the potentially observed effect. On the other side, it significantly increased the accumulated statistics. The latter was a more important consideration during the experiment, as the main goal was to observe the effect, but not to measure its absolute value. This approach has been successfully proved in our last measurement on the ROT effect [8].

6 Performance evaluation

The accuracy of the described experimental technique is determined by systematic and statistical errors. We can distinguish three main sources of systematic errors which could simulate the effect.

1) The influence of the magnetic field of the spin-control devices on the PMT, that are part of the neutron and γ-ray detectors. To minimize the magnetic field influence, neutron and γ-ray detectors were shielded by mu-metal. In addition, passive monitoring of this effect was carried out - the counting speed asymmetry of detectors was measured without coincidence with FF (that is, the background of γ-rays and neutrons). This asymmetry did not exceed 10^{-5}.

2) The influence of the spin flipper switching on a data processing system. Spin flipper switching was controlled by modules located in NIM crates. Optical cables were used to reduce this effect. Monitoring was carried out by measuring the FF detectors count rate. A statistically significant difference from the zero asymmetry of the FF count was observed only during the periods of neutron beam intensity abrupt change, due to a change in reactor power. Exposures with this asymmetry were ignored during data processing. The average asymmetry did not exceed 10^{-5}.

3) The data collection time asymmetry for opposite directions of neutron beam polarization. This time was set by a quartz generator and controlled by another quartz generator. The data collection time asymmetry did not exceed 10^{-6} during the measurements.

Statistical error is determined by the amount of collected data. The data collection speed with the used technique (per unit time) is limited by the dead time of the electronics and the influence of random coincidences. The maximum achievable statistical accuracy is about 10^{-3} for the data set collected within 1 second. It is possible to reach a statistical accuracy of about 10^{-5} during 30 days of continuous measurements.

Figure 13 shows the result of the measurement of gamma ROT-asymmetries in an isolated resonance of ^{235}U induced by polarized neutron beam with an energy of 270 meV. The value of the

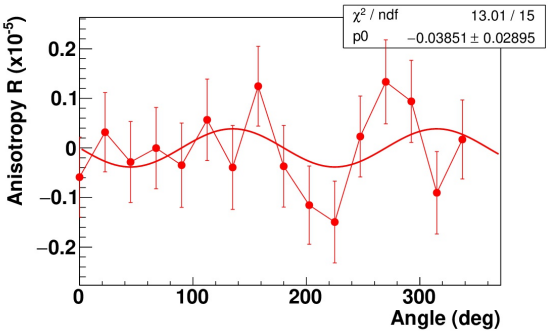

Figure 13. Anisotropy ratio R as a function of angle for the gamma-rays.

asymmetry is calculated by the formula:

$$R = \frac{N_+ - N_-}{N_+ + N_-}$$

Here N_+ and N_- are the coincidence count rates for opposite directions of the neutron polarization. The angular dependence at first approximation is fitted by the function $F = A \cdot sin(2\theta)$, which is shown on the plots. The anisotropy parameter A is determined from the fit and equals to A_γ=(-3.8±2.8)×10^{-5} , χ^2/N being 0.87 . The results of this experiment are in agreement with the most modern theoretical model prediction proposed in [8].

7 Conclusion

An apparatus for studying ROT- and TRI- asymmetries in neutron-induced nuclear fission with short wavelength neutrons (energies close to the first resonance of the heavy nucleus) was successfully built and tested. It uses intense non-polarized neutron beams from variably double-focused monochromators on instrument POLI at MLZ in combination with ^3He spin filter polarizers in order to reach a large cross section polarized neutron beam with high flux intensity (> 10^6 n(s· $cm^2)^{-1}$) at different energies. It consists polarizing/analyzing devices, spin transport and manipulation system, fission chamber including of detectors for neutrons, γ-rays, and fission fragments, as well as studied target, electronics and data acquisition systems. The apparatus run fast on a Linux OS. The system allows only the data recording, while the data processing is supposed to be performed off-line. A test run for the complete setup was successfully performed with ^{235}U target and polarized neutrons with energy of 270 meV corresponding to the lowest resonance for that isotope. The experimental results showed that the apparatus works well and the data analysis method was established for the experimental results. Running in synchronization mode, the system provided information about FF, prompt fission γ-rays and neutrons, spin states, neutron depolarization etc.

The TOF method with plastic scintillation detectors was successfully tested using the "start" signals from the FF detectors. The observed TOF spectra of the plastic scintillators provided good neutron-gamma discrimination due to the sufficient distance and the solid angle between the detectors. NaI scintillators were used due to their high γ-ray detection efficiency, in spite the lower TOF spectra accuracy.

The results of the test experiments show that using described apparatus and optimized parameters a statistical accuracy in the experimentally determined asymmetries of the ROT and TRI effects at the level of 10^{-4} could be reached within about one week of beam-time only. Thus, it provides the basis for the systematic routine investigation of those effects in different heavy isotopes in the future.

Acknowledgments

This work has been supported by the Russian Ministry for Science and Education, German Ministry for Education and Research BMBF through the project 05K13PA3. The instrument POLI is operated by RWTH Aachen in cooperation with JCNS FZ Jülich (Jülich Aachen Research Alliance JARA). We're grateful to K. Lehmann, A. Sazonov, W. Luberstetter, and P. Stein for their help in setting up and conducting the experiment.

References

[1] P. Jesinger, G. V. Danilyan, A. M. Gagarski, et al., *Interference effect in the angular distribution of outgoing particles in ternary fission induced by cold polarized neutrons*, *Phys. At. Nucl.* **62** (1999) 1608.

[2] P. Jesinger, A.Kotzle, A.Gagarski et al., *Observation of a triple correlation in ternary fission: is time reversal invariance violated?*, *Nucl. Instrum. Methods Phys. Res. A* **440** (2000) 618.

[3] K. Schreckenbach, J. van Klinken, and J. Last, *TRI Tests by Internal Pair Production Following Polarized Neutron Capture*, *in Proceedings of the Conference on Time Reversal Invariance and Parity Violation in Neutron Reactions, Dubna, Russia, May 4-7,1994*.

[4] P. Jesinger, A.Kotzle, F. Goennenwein et al., *Angular Correlations in Ternary Fission Induced by Polarized Neutrons*, *Phys. At. Nucl.* **65** (2002) 630.

[5] F. Goennenwein, M. Mutterer, A. Gagarski et al., *Rotation of the compound nucleus* $236U*$ *in the fission reaction* $235U(n, f)$ *induced by cold polarised neutrons*, *Pys. Let. B* **652** (2007) 13.

[6] F. Goennenwein, A. Gagarski, G. Petrov et al., *Tri and Rot effects in ternary fission: What can be learned?*, *AIP Conference Proceedings* **1224** (2010) 338.

[7] A. Gagarski F. Goennenwein, I.Guseva et al., *Particular features of ternary fission induced by polarized neutrons in the major actinides* $233, 235U$ *and* $239, 241Pu$, *Phys. Rev. C* **93** (2016) 054619.

[8] Yu. Kopatch, V.Novitsky, G.Ahmadov et al., *Measurement of the ROT effect in the neutron induced fission of* $235U$ *in the* $0.3eV$ *resonance at a hot source of polarized neutrons*, *EPJ Web of Conf.* **169** (2018) 00010.

[9] V. Hutanu, M. Meven and G. Heger, *Construction of the new polarised hot neutrons single-crystal diffractometer POLI-HEiDi at FRM-II*, *Physica B: Condensed Matter* **397** (2007) 135.

[10] V. Hutanu, M. Meven, E. Lelievre-Berna and G. Heger, *POLI-HEiDi: The new polarised neutron diffractometer at the hot source (SR9) at the FRM II - Project status*, *Physica B* **404** (2009) 2633.

[11] V. Hutanu, *POLI: Polarised hot neutron diffractometer*, *Journal of large-scale research facilities* **1** (2015) A16.

[12] Hutanu V, Masalovich S, Meven M, Lykhvar O, Borchert G and Heger G, *Scientific Review: Polarized* ^{3}*He Spin Filters for Hot Neutrons at the FRM II*, *Neutron News* **18** (2007) 14.

[13] Lelievre-Berna E and Tasset F, *The D3C project: improvements and new fields of science*, *Physica B: Condensed Matter* **267** (1999) 21.

[14] V. Hutanu, M. Meven, S. Masalovich, G. Heger, and G. Roth, *3He spin filters for spherical neutron polarimetry at the hot neutrons single crystal diffractometer POLI-HeiDi*, *J. Phys.: Conf. Ser.* **294** (2011) 012012.

[15] V. Hutanu, M. Meven, A. Sazonov and G. Heger, *Development of compact magnetostatic cavities for 3He spin filter cells*, *Meas. Sci. Technol.* **19** (2008) 034010.

[16] Masalovich S, *Method to measure neutron beam polarization with 2×1 Neutron Spin Filter*, *Nucl. Inst. and Meth. A* **581** (2007) 791.